H5N8 and H7N9 packaging signals constrain HA reassortment with a seasonal H3N2 influenza A virus

Maria C. White[a], Hui Tao[a], John Steel[a], and Anice C. Lowen[a,1]

[a]Department of Microbiology and Immunology, Emory University School of Medicine, Atlanta, GA 30322

Edited by Peter Palese, Icahn School of Medicine at Mount Sinai, New York, NY, and approved January 17, 2019 (received for review October 26, 2018)

Influenza A virus (IAV) has a segmented genome, which (*i*) allows for exchange of gene segments in coinfected cells, termed reassortment, and (*ii*) necessitates a selective packaging mechanism to ensure incorporation of a complete set of segments into virus particles. Packaging signals serve as segment identifiers and enable segment-specific packaging. We have previously shown that packaging signals limit reassortment between heterologous IAV strains in a segment-dependent manner. Here, we evaluated the extent to which packaging signals prevent reassortment events that would raise concern for pandemic emergence. Specifically, we tested the compatibility of hemagglutinin (HA) packaging signals from H5N8 and H7N9 avian IAVs with a human seasonal H3N2 IAV. By evaluating reassortment outcomes, we demonstrate that HA segments carrying H5 or H7 packaging signals are significantly disfavored for incorporation into a human H3N2 virus in both cell culture and a guinea pig model. However, incorporation of the heterologous HAs was not excluded fully, and variants with heterologous HA packaging signals were detected at low levels in vivo, including in naïve contact animals. This work indicates that the likelihood of reassortment between human seasonal IAV and avian IAV is reduced by divergence in the RNA packaging signals of the HA segment. These findings offer important insight into the molecular mechanisms governing IAV emergence and inform efforts to estimate the risks posed by H7N9 and H5N8 subtype avian IAVs.

influenza A virus | reassortment | packaging | zoonosis | antigenic shift

Influenza A virus (IAV) exhibits a broad host range, including wild birds, poultry, and humans (1). The segmented nature of the IAV genome allows for gene segments to be exchanged through reassortment in coinfected cells (2). This process contributes to both pandemic and epidemic influenza; notably, reassortment involving IAVs adapted to differing host species played a critical role in the formation of the last three IAV pandemic strains (3–5). Antigenic novelty is a key feature of IAV pandemics and is achieved through the introduction of a novel HA, which can be facilitated by reassortment. As such, reassortment of human IAV with avian IAV presents a pandemic risk. Zoonotic transmission of avian IAVs of the H5N1 and H7N9 subtypes has caused multiple outbreaks of severe disease in humans over the last two decades (6–8). H5N8 subtype viruses, while yet to cause disease in humans, derive the HA segment from the influenza A/goose/Guangdong/1/96 (H5N1) lineage associated with zoonosis (9). Since emergence and global expansion of the H5Nx lineage in 2014, this poultry-adapted H5 HA has reassorted extensively with IAVs circulating in wild waterfowl, and the resultant viruses have caused major outbreaks in poultry (10–12). The exposure of humans at the animal–human interface to H5Nx and H7N9 viruses engenders a risk of avian–human IAV reassortment. Importantly, however, the genetic compatibility of these avian viruses with human seasonal IAVs remains poorly understood.

Here we sought to address this knowledge gap by evaluating the compatibility of H5N8 and H7N9 genetic components with those of a seasonal H3N2 virus, focusing on the RNA packaging signal regions of the HA segment. IAV packaging signals direct the incorporation of the eight gene segments into virus particles, and have previously been shown by us and others to influence reassortment outcomes between different IAV strains (13–15). In this study, we assessed the compatibility of HA packaging signals originating from H5N8 and H7N9 subtype IAVs with a seasonal H3N2 strain background. We isolated the effects of the RNA packaging signals by generating chimeric viruses that retained the coding capacity of the seasonal H3N2 strain but included the terminal packaging signal regions derived from H5 or H7 HA segments. We then determined the frequency with which HA segments carrying homologous vs. heterologous packaging signals were taken up during reassortment. Our data show that H5N8 and H7N9 HA packaging signals (HA_H5PS and HA_H7PS, respectively) are disfavored for reassortment into the H3N2 strain background to varying degrees in both MDCK cells and a guinea pig model. In guinea pigs coinfected with HA_H3PS plus HA_H5PS, HA segments carrying H5N8 packaging signals were transmitted to a subset of naïve contacts, while in animals coinoculated with HA_H3PS plus HA_H7PS viruses, HA segments with the H7N9 packaging signals showed very limited transfer to contacts. These data indicate that the packaging signals of H5 and H7 HA segments constrain reassortment with a seasonal H3N2 virus. Importantly, however, exclusion of heterologous packaging signals was not complete, suggesting that reassortment of H5 or H7 HA segments into seasonal H3N2 backgrounds is likely to proceed at an appreciable level in coinfected hosts. Incompatibilities at the RNA level were also not sufficiently strong to fully prevent propagation of these reassortants to contacts.

Significance

Influenza A viruses (IAV) can exchange genetic material in coinfected cells in a process termed reassortment. The last three IAV pandemic strains arose from reassortment events involving human and nonhuman IAVs. Because introduction of the hemagglutinin (HA) gene from a nonhuman virus is required for a pandemic, we addressed the compatibility of human and avian IAV. We show that sequence differences between human and avian HA genes limit the potential for reassortment. However, human IAV still incorporated heterologous HA genes at a low level in coinfected animals. This observed low level of incorporation could become significant if reassortant viruses had a fitness advantage within the host, such as resistance to preexisting immunity, and highlights the continued need for IAV surveillance.

Author contributions: M.C.W., J.S., and A.C.L. designed research; M.C.W. and H.T. performed research; J.S. contributed new reagents/analytic tools; M.C.W. and A.C.L. analyzed data; and M.C.W. and A.C.L. wrote the paper.

The authors declare no conflict of interest.

This article is a PNAS Direct Submission.

[1]To whom correspondence should be addressed. Email: anice.lowen@emory.edu.

This article contains supporting information online at www.pnas.org/lookup/suppl/doi:10.1073/pnas.1818494116/-/DCSupplemental.

Published online February 13, 2019.

Results

Chimeric HA Segments for Quantifying Mismatch Among Packaging Signals. To measure constraints on reassortment imposed at the level of packaging, we generated a panel of HA segments that differed only in the packaging signals. Each segment encoded the influenza A/Panama/2007/99 (H3N2; Pan/99) HA protein but carried terminal packaging signals from influenza A/mute_swan/Croatia/70/2016 (H5N8), influenza A/Anhui/1/2013 (H7N9), or Pan/99 viruses (*SI Appendix*, Fig. S1 *A–D*). These packaging signals were introduced upstream and downstream of the ORF, effectively lengthening the untranslated regions (UTRs) of the HA segments. To disrupt native packaging function in the Pan/99 ORF, we silently mutated the terminal 20 codons at the 5′ and 3′ ends, as in ref. 16. As a control to verify disruption of native packaging function, we also produced a Pan/99 HA segment with these silent mutations in the ORF and no introduced packaging signals, termed PSmut_HA (*SI Appendix*, Fig. S1*E*).

We generated virus pairs using our Pan/99 WT-variant (VAR) system, designed to track the origins of segments in reassortant progeny (15, 17) (*SI Appendix*, Fig. S2*A*). The VAR virus contains silent genetic tags, while the WT virus is untagged. We allowed the PSmut_HA virus to coinfect MDCK cells with a Pan/99 VAR virus containing intact packaging signals on HA and measured the frequency with which each HA segment was incorporated into reassortant progeny by screening plaque isolates. Results showed that packaging of the PSmut_HA segment was significantly disfavored, confirming disruption of ORF packaging function (*SI Appendix*, Fig. S2 *B* and *C*). We also confirmed that the PSmut_HA segments were replicated efficiently by the viral polymerase (*SI Appendix*, Fig. S2 *D* and *E*).

Viruses with Modified Packaging Signals Did Not Differ in Growth. To determine if the introduced packaging signals altered viral growth, we first analyzed single-cycle replication in MDCK cells with our HA segment-modified viruses (*SI Appendix*, Fig. S1 *A–D*) and Pan/99 virus as a control. Over the course of 24 h, all viruses displayed similar growth kinetics, indicating that the packaging signal modifications did not suppress virus growth (*SI Appendix*, Fig. S3*A*). We next analyzed multicycle growth of a subset of these viruses in guinea pigs. Growth of all viruses was similar in vivo, further substantiating that the introduced packaging signal modifications had minimal impact on virus growth (*SI Appendix*, Fig. S3*B*).

Chimeric Pan/99 HA Segments Were Replicated Efficiently. To assess replication of the modified HA segments within coinfected cells, we used a RT droplet digital PCR (ddPCR) assay to enumerate total copies of each of the HA segments present in coinfected cells and matched supernatants. Replication of the HA segments carrying Pan/99 packaging signals (HA_H3PS) and H7N9 packaging signals (HA_H7PS) were equal over time except at the 10-h time point, where more of the HA_H7PS segment was detected (*SI Appendix*, Fig. S4). Replication of the HA_H3PS segment was slightly more efficient than replication of the HA segment carrying H5N8 packaging signals (HA_H5PS) (*SI Appendix*, Fig. S4).

HA Segments Carrying H5N8 or H7N9 Packaging Signals Were Disfavored for Incorporation into a H3N2 Background. To determine if heterologous H5 or H7 HA packaging signals limited reassortment, we coinfected MDCK cells with WT-VAR virus pairs that differed only in the packaging signal regions on the HA segment (Fig. 1 *A–C*). After a single cycle of replication, we harvested the supernatants and genotyped reassortant progeny. We performed coinfections under two different conditions for the HA_H3PS plus HA_H5PS virus pairing to account for the differences in HA segment replication observed in *SI Appendix*, Fig. S4. Under all conditions tested, the heterologous HA_H5PS and HA_H7PS segments were significantly underrepresented in reassortant progeny (Fig. 1 *D–F*). However, in coinfections performed in parallel under 1:1 WT:VAR input conditions, the HA_H7PS segment was packaged more frequently than the HA_H5PS segment (Fig. 1 *D* and *F*). Taken together, these data suggest that HA segments carrying H5N8 or H7N9 packaging signals are not efficiently incorporated into a human seasonal H3N2 background, but that H7N9 HA packaging signals exhibit a lower incorporation barrier.

HA Segments Carrying H5N8 or H7N9 Packaging Signals Were Not Incorporated as Efficiently as Homologous Segments in Coinfected Guinea Pigs. To determine if the phenotypes observed in cell culture were also observed in vivo, we coinfected female guinea pigs with our modified viruses as shown in Fig. 1 *B* and *C*. At 16 h postinoculation (p.i.), a naïve guinea pig was cocaged with each inoculated animal. Nasal lavage was performed daily over a 7-d time course to determine virus titers. Viruses grew in all inoculated animals, and all contacts contracted infection (*SI Appendix*, Fig. S5). Nasal washes from each inoculated animal at 2 d and 4 d p.i. were processed for reassortment analysis. Parental VAR genotypes were more abundant than parental WT genotypes in the inoculated animals despite slight overrepresentation of WT virus in the inocula (Fig. 2 and *SI Appendix*, Fig. S6). This observation suggests that the heterologous packaging signals on the HA of both WT viruses hindered virus propagation in vivo when in competition with a better-matched (VAR) virus. Analysis of the reassortant progeny revealed that, at both time points, the HA_H5PS segment was packaged significantly less frequently than the HA_H3PS segment (Fig. 3 *A–D*), confirming the results obtained in cell culture. Results for the HA_H3PS plus HA_H7PS coinfection showed there was no preference for either HA segment at 2 d p.i., but 4 d p.i. revealed a significant preference for HA_H3PS (Fig. 3 *E–H*). Thus, reassortment analyses again supported the results obtained in cell culture. In contrast to examination of viral growth during single infections in cell culture and in vivo, however, the predominance of parental VAR genotypes in vivo under coinfection conditions suggested that the presence of heterologous packaging signals on HA is detrimental to propagation when in competition with a virus that carries homologous packaging signals on HA.

HA Segments Carrying H5N8, but Not H7N9, Packaging Signals Were Transmitted. Next, we evaluated which HA segments were transmitted to the naïve cage mates and how long these HA segments persisted in the host over time. We used primers specific for the 3′ HA packaging signal region in a RT ddPCR assay to determine copy numbers of each modified HA segment over time in the nasal washings of contact animals. We found that, in all eight contact animals, the HA_H3PS segment was abundant, and copy numbers correlated with infectious titers (Fig. 4 *A* and *C*). We were able to robustly detect HA_H5PS in two of the four exposed guinea pigs at multiple time points, and, in one animal, total copies of HA_H5PS exceeded the total copies of HA_H3PS at 5 d p.i. (Fig. 4*B*). In contrast, robust detection of the HA_H7PS segment was not observed in any of the exposed guinea pigs (Fig. 4*D*), suggesting that neither the Pan/99 HA_H7PS parental virus nor reassortant viruses carrying the HA_H7PS segment were shed at sufficient levels to transmit in the context of a contact transmission model. We validated these findings by repeating the transmission experiment a second time. In this second experiment, fresh aliquots of the same WT-VAR mixtures analyzed in Fig. 2 and *SI Appendix*, Fig. S6 were used for inoculation. In all eight inoculated animals, both WT and VAR HA segments were detected at 2 d p.i., but, as before, the VAR HA_H3PS predominated (*SI Appendix*, Fig. S7 *A–D*). In all eight contact animals the HA_H3PS segment was abundant over time, with kinetics similar to the first experiment (*SI Appendix*, Fig. S7 *E* and *G*). We were again able to robustly detect

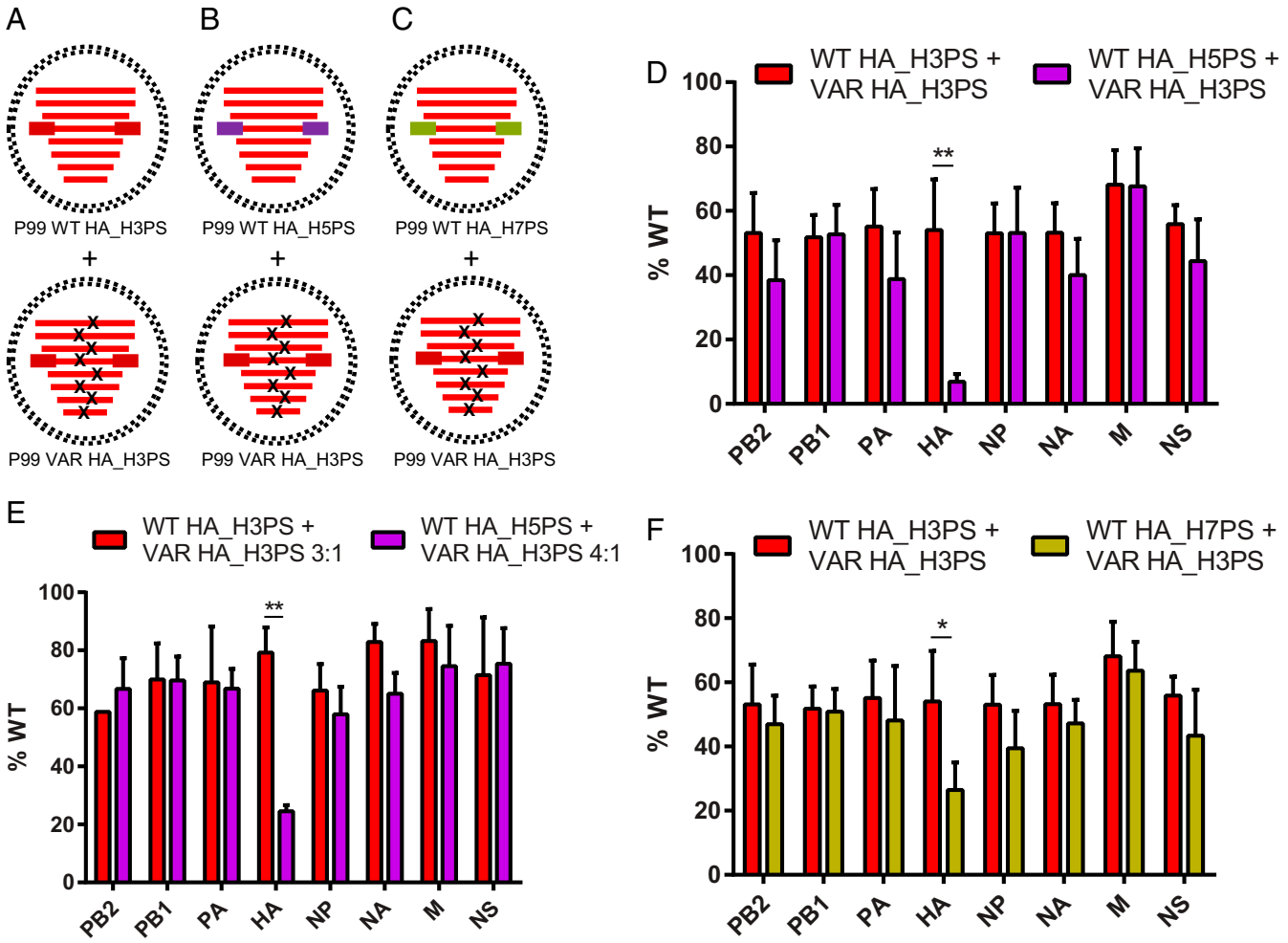

Fig. 1. HA segments carrying H5 or H7 packaging signals constrained reassortment with H3N2 viruses in cell culture. (*A–C*) Coinfections were performed using virus pairs that contained modified HA segments in a Pan/99 background. Within each pairing, one virus, designated as VAR, contained silent genetic tags (x's), while the other virus was untagged (WT). The control virus pairing in *A* carried homologous H3N2 packaging signals on the HA of both viruses (red boxes). For the heterologous coinfections, the WT virus carried either H5N8 (purple boxes) or H7N9 (gold boxes) packaging signals on HA, while the VAR virus carried homologous H3N2 packaging signals (*B* and *C*, respectively). (*D–F*) MDCK cells were coinfected with the indicated viruses at a high MOI. Supernatants were harvested 12 h p.i., and virus isolates were genotyped via HRM analysis. The percentage of virus isolates that carried a WT segment for each of the eight IAV segments is shown. Only reassortant virus isolates were included in the analysis. (*D* and *F*) Input ratios of 1:1 WT:VAR were used, and $n = 6$ for each coinfection (two biological replicates performed in triplicate). The control dataset shown in both panels is the same, and all three coinfections were performed in parallel. (*E*) Input ratio of 3:1 WT:VAR for the control coinfection and 4:1 WT:VAR for the heterologous coinfection were used, and $n = 3$ (one biological replicate performed in triplicate). Data are plotted as mean with SD. $^{**}P < 0.0001$, $^{*}P = 0.0032$ using two-way ANOVA with Tukey's multiple comparisons.

HA_H5PS in two of the four exposed guinea pigs at multiple time points (*SI Appendix*, Fig. S7*F*) and observed minimal HA_H7PS transfer to contacts with no robust replication (*SI Appendix*, Fig. S7*H*). Thus, results of this second transmission experiment closely matched the results of the first experiment. The data suggest that HA segments carrying H5N8 or H7N9 packaging signals are not efficiently transmitted within a human seasonal H3N2 background, but that H5N8 HA packaging signals functioned slightly better than the H7N9 packaging signals in this regard.

HA Segments Carrying H5N8 or H7N9 Packaging Signals Were Present Less Frequently than Pan/99 HA Segments in Virus Particles. Our reassortment data obtained from coinfected cells clearly indicated that, when in direct competition, HA_H3PS was more efficiently incorporated into the H3N2 background than HA segments carrying either H5 or H7 packaging signals. To test the extent to which competition during genome assembly contributes to this phenotype, we evaluated the efficiency with which each HA segment was packaged into particles during standard propagation of the individual viruses. Thus, we concentrated HA_H3PS, HA_H5PS, HA_H7PS, and control Pan/99 viruses grown in eggs through a sucrose cushion and used RT ddPCR to measure HA segment copy numbers in the resultant virus preparations. We saw no significant difference between HA segment copy number in the HA_H3PS virus preparation compared with the control Pan/99 virus with no packaging signal modifications (Fig. 5 *A* and *B*). In contrast, the HA segment in the HA_H5PS virus was present significantly less frequently. The HA of the HA_H7PS virus was also low compared with the Pan/99 control, but significance varied with the primer set used (Fig. 5 *A* and *B*). These data suggest that, even in the absence of competition between HA segments within a coinfected cell, the presence of H5 or H7 packaging signals on HA lowers packaging efficiency into a Pan/99 virus. We then extended these analyses to include all eight IAV segments and noted modest packaging defects for a handful of non-HA segments (Fig. 5*C*).

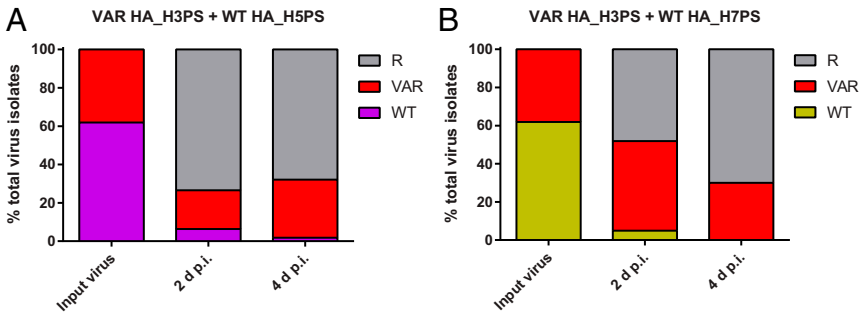

Fig. 2. Heterologous packaging signals on the HA segment of both WT viruses hindered virus propagation in coinfected guinea pigs. Guinea pigs were inoculated with a 1:1 WT:VAR virus mixture consisting of HA_H3PS plus HA_H5PS (*A*) or HA_H3PS plus HA_H7PS viruses (*B*). Genotyping was performed on the input virus and virus isolates sampled from the inoculated animals at 2 and 4 d p.i. Data from all four guinea pigs in each group are pooled. (*A*) $n = 21$ virus isolates for the input virus, $n = 79$ virus isolates for 2 d p.i., and $n = 56$ virus isolates for 4 d p.i. (*B*) $n = 21$ virus isolates for the input virus, $n = 81$ virus isolates for 2 d p.i., and $n = 80$ virus isolates for 4 d p.i. The reassortant isolates in *A* and *B* are the same isolates analyzed in Fig. 3. R, reassortant genotype; VAR, parental VAR genotype; WT, parental WT genotype.

Discussion

This study aimed to determine HA packaging signal compatibility between a human H3N2 virus and zoonotic H5N8 and H7N9 viruses. We previously showed that HA segments carrying homologous H3N2 packaging signals were significantly preferred for packaging into H3N2 viruses over HA segments carrying heterologous H1N1 packaging signals (15). We sought to test this concept for other IAV strain pairings, particularly those which carry pandemic potential. We isolated the effects of packaging signals on reassortment by designing virus pairs that retained H3N2 protein-coding capacity but differed in the packaging signals on the HA segment. Our results showed that HA segments carrying homologous H3N2 packaging signals were taken up into reassortant viruses significantly more frequently than HA segments carrying H5N8 or H7N9 packaging signals, extending previous observations of packaging signal constraint on reassortment to viruses that present a pandemic risk (13, 14). This phenotype was observed in both MDCK cells and guinea pigs. Importantly, onward transmission of HA segments carrying heterologous packaging signals occurred with low efficiency from coinfected guinea pigs, underlining the fitness implications of packaging signal mismatch. It is noteworthy, however, that HA segments carrying H5 packaging signals were consistently detected in a subset of the naïve contacts of coinfected animals, while minimal transfer of HA_H7PS segments to contacts was detected. These findings suggest that H5 packaging signals are sufficiently compatible with H3N2 viruses to allow a low level of transmission.

Reassortment can facilitate host species transfer of IAVs, and reassortment between human and avian IAV is of particular concern for the emergence of novel pandemic strains (18). Areas such as backyard poultry farms and live bird markets, where humans are in close contact with poultry, provide an environment

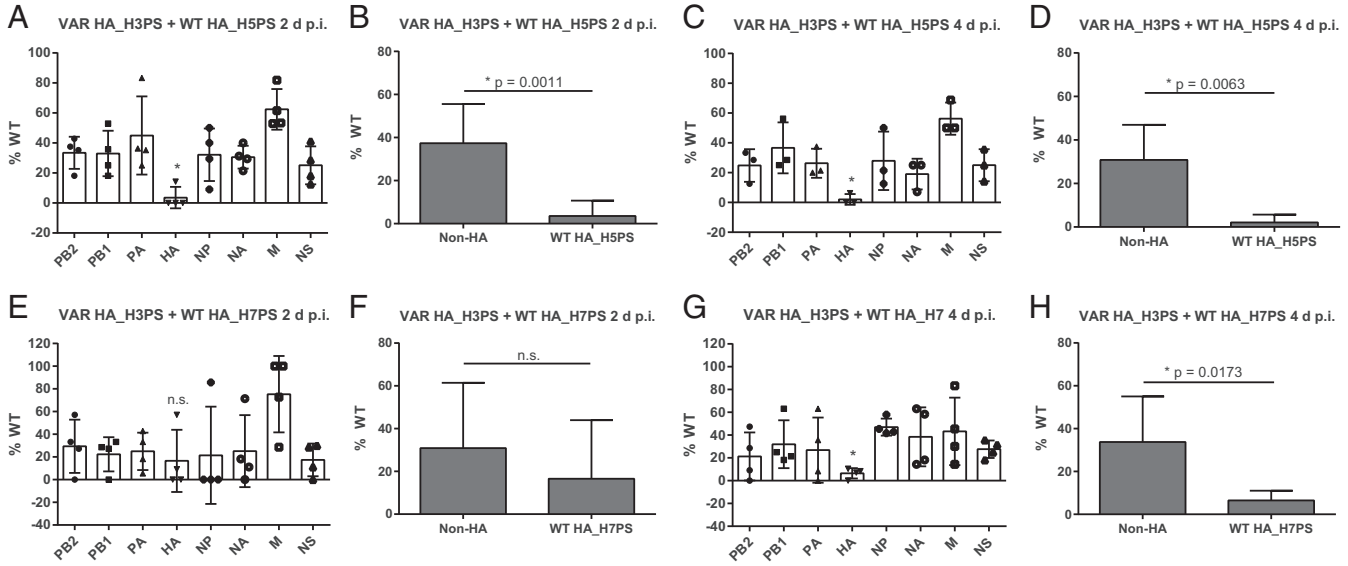

Fig. 3. H5 or H7 packaging signals limited HA reassortment with H3N2 viruses in coinfected animals. Guinea pigs were coinfected with either HA_H3PS plus HA_H5PS viruses (*A–D*) or HA_H3PS plus HA_H7PS viruses (*E–H*), and viruses sampled by nasal lavage at 2 d p.i. (*A*, *B*, *E*, and *F*) and 4 d p.i. (*C*, *D*, *G*, and *H*) were genotyped via HRM analysis. The percentage of virus isolates that carried a WT gene segment for each of the eight IAV segments is plotted on the *y* axis. The WT HA segment in each coinfection carried heterologous (H5 or H7) packaging signals. Only reassortant virus isolates were included in the analysis (same reassortant isolates reported in Fig. 2). Each data point represents one animal: $n = 4$ animals for *A*, $n = 3$ animals for *C*, $n = 4$ animals for *E*, and $n = 4$ animals for *G*. (*B*, *D*, *F*, and *H*) Unpaired *t* test was used to analyze the difference between % WT for the modified HA segment vs. unmodified (non-HA) segments for each reassortment dataset. All data are plotted as mean with SD. Calculated *P* values are displayed on the graphs; n.s., not significant. Indications of significance in *A, C, E,* and *G* are derived from the corresponding analyses in *B, D, F,* and *H*.

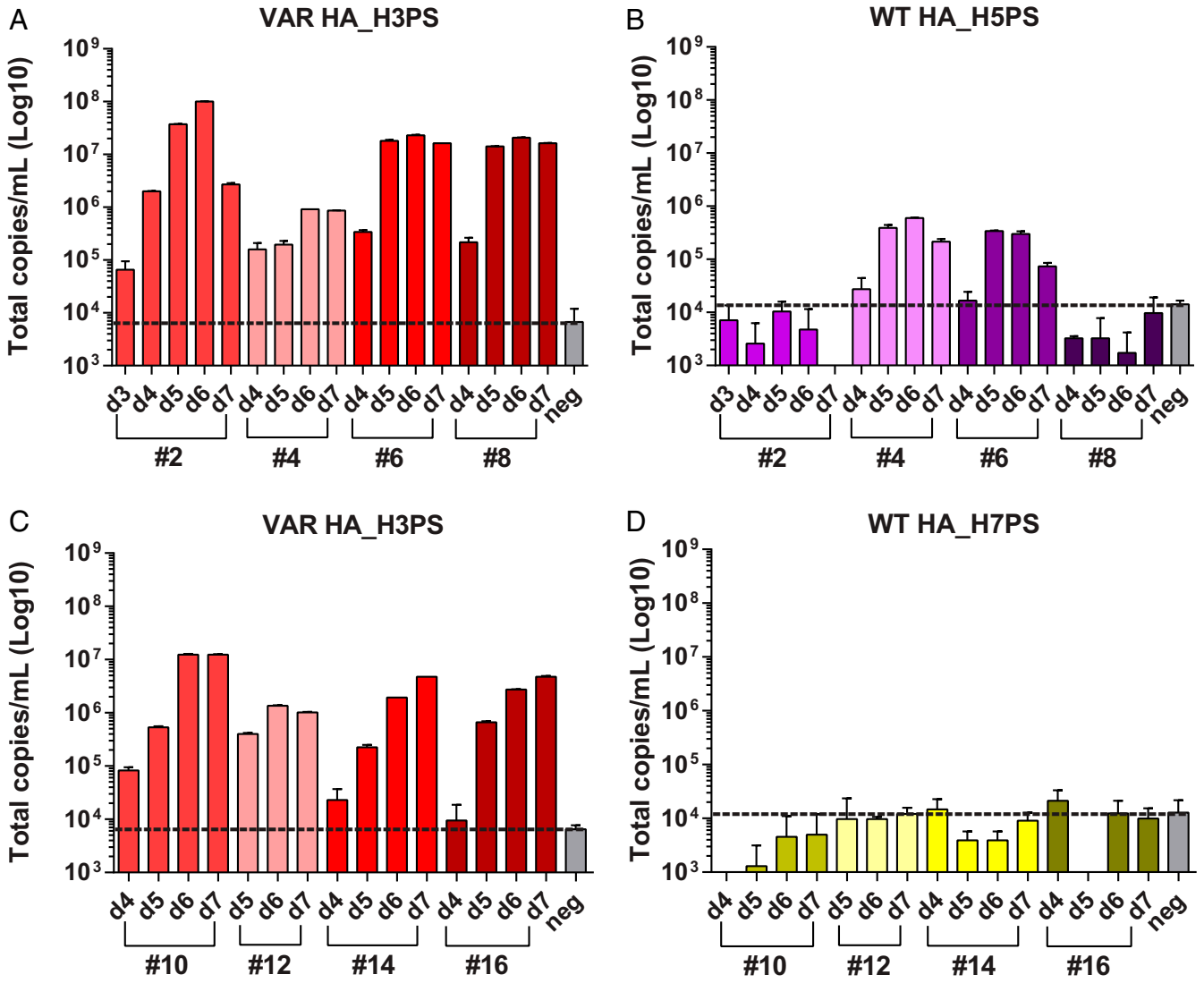

Fig. 4. HA segments carrying H5, but not H7, packaging signals were transmitted to naïve contact animals. Nasal wash fluid of animals exposed to coinfected guinea pigs was analyzed by RT ddPCR to detect HA segment transmission. Primers specific to the 3′ packaging signal of each HA segment were used, and each reaction was performed in duplicate. The day of sampling is shown on the *x* axis, and guinea pig ID numbers are indicated underneath. The background values of the assay (measured using primer + dH2O) were used to define the negative (neg), which is represented by a dotted black line. (*A* and *B*) Animals exposed to HA_H3PS plus HA_H5PS coinfected animals. (*C* and *D*) Animals exposed to HA_H3PS plus HA_H7PS coinfected animals. Data are plotted as mean with SD.

where human and avian IAVs could coinfect and undergo reassortment (19). We previously showed that reassortment occurs readily when coinfecting IAVs are highly homologous (17). Constraints on reassortment can arise, however, due to incompatibilities between heterologous viruses at both the RNA and protein levels (reviewed in ref. 20). This phenomenon of segment mismatch is complex, owing to negative epistasis involving multiple components simultaneously. Our data show that HA packaging signal mismatch disfavors, but does not completely prevent, the formation of genotypes containing HA H5N8 or H7N9 packaging signals. The production of these heterologous genotypes at low levels could be significant in contexts where HA reassortant viruses possess a fitness advantage over other variants, such as in hosts with preexisting immunity. The extent of HA protein mismatch between human and avian IAV would offer additional insights into the potential for reassortants to be propagated once formed.

Notably, we observed a higher incorporation barrier for HA segments carrying H5 compared with H7 packaging signals. A possible explanation for this observation is the increased phylogenetic relatedness of H3 and H7 subtypes. IAV HA genes are divided phylogenetically into two major groups (21). Group 1 includes H1 and H5, while group 2 includes H3 and H7. Given our current and past findings using H1, H3, H5, and H7 packaging signals, it is tempting to speculate that an H3N2 virus such as Pan/99 would more readily incorporate H7 packaging signals than H1 or H5 packaging signals due to higher HA sequence conservation. However, more HA subtype pairings would be needed to robustly test this hypothesis. The nucleotide identity between the H3N2 vs. H5N8 and H3N2 vs. H7N9 IAV strains used in this study are 52.9 and 56.6%, respectively, in the HA packaging signal regions as defined herein. While H3 and H7 share slightly higher identity than H3 and H5 in these regions, the significance of this difference is difficult to predict given the lack of knowledge surrounding which nucleotides are important for mediating HA segment packaging.

In our animal study, despite there being more WT (heterologous HA_PS) than VAR (homologous HA_PS) virus in both of the coinfection inocula, the VAR virus strongly predominated over WT in nasal lavage samples. This phenotype was most

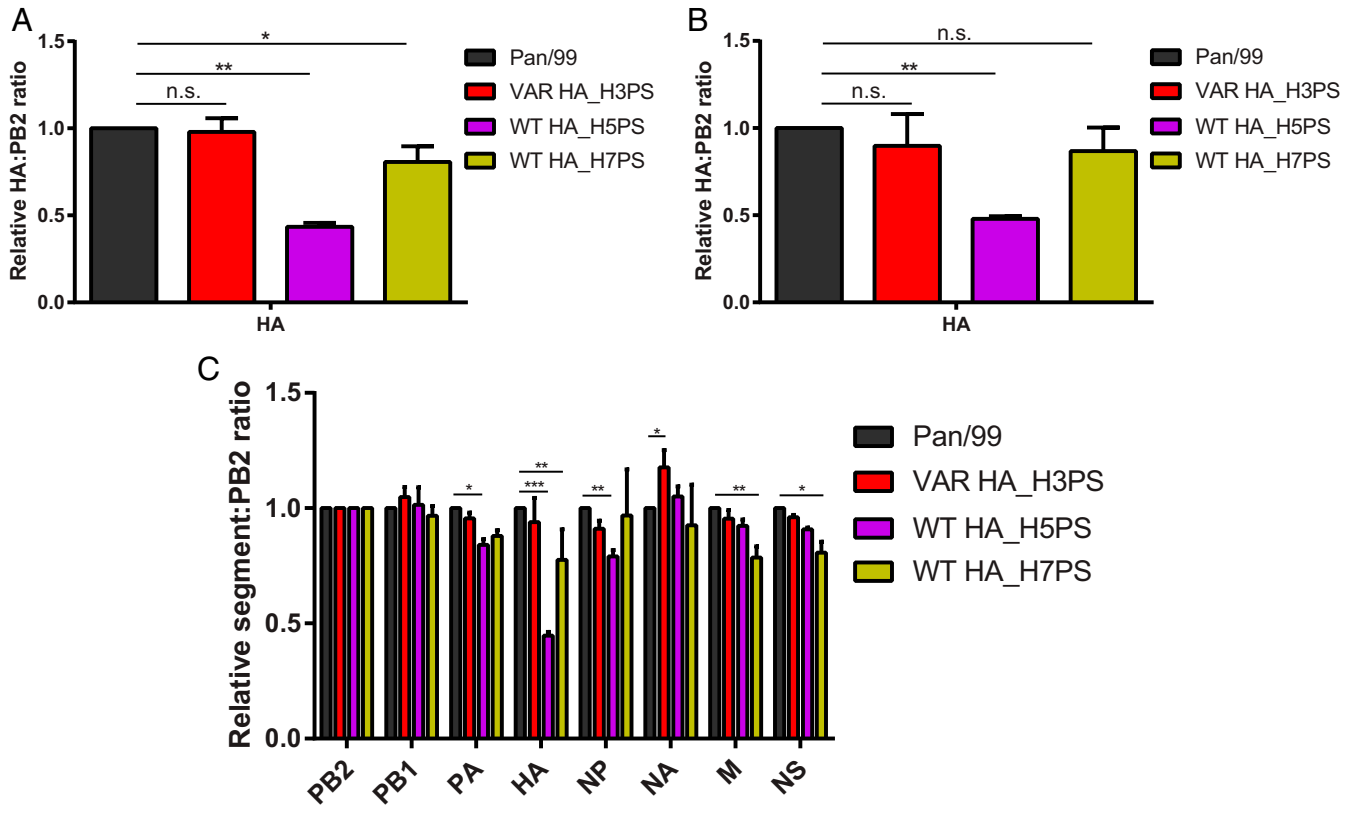

Fig. 5. HA segments carrying H5 or H7 packaging signals were present less frequently than control Pan/99 HA segments in virus particles. Triplicate stocks of HA_H3PS, HA_H5PS, HA_H7PS, and control Pan/99 viruses were grown in embryonated eggs. Each of the resultant 12 stocks was processed individually by concentration through a sucrose cushion. RT ddPCR was used to enumerate segment copy number in the resultant virus preparations. (*A* and *B*) HA copy numbers were normalized to PB2 copy numbers and then normalized to the control Pan/99 values. $n = 3$ for each virus (three technical replicates with ddPCR performed in duplicate for each). Independent sets of PB2 and HA primers were used to generate data shown in *A* and *B*. Data are plotted as mean with SD and analyzed using one-way ANOVA with Dunnett's multiple comparisons. (*A*) $^{**}P < 0.0001$, $^{*}P = 0.0119$, n.s., not significant; (*B*) $^{**}P = 0.0013$, n.s., not significant. (*C*) All segment copy numbers were normalized to PB2 copy numbers and then normalized to the control Pan/99 values. $n = 3$ for each virus (three technical replicates with ddPCR performed in duplicate for each). HA data were acquired using the primer set in *A* and at a separate time from the remaining seven segments. Data are plotted as mean with SD and analyzed within segments using two-way ANOVA with Dunnett's multiple comparisons; $^{***}P < 0.0001$, $^{**}P < 0.0005$, $^{*}P < 0.01$.

striking in the HA_H3PS plus HA_H7PS inoculated animals, where the parental VAR isolates also outnumbered reassortants at 2 d p.i. The relative levels of WT, VAR, and reassortant genotypes detected suggest linkage among the eight segments is maintained early during infection by a relative lack of reassortment. In this situation, the VAR virus would be expected to maintain a fitness advantage because the HA segment in the VAR system carries homologous packaging signals. This outgrowth of VAR virus in the HA_H3PS plus HA_H7PS inoculated animals may have contributed to the lack of a packaging phenotype at 2 d p.i. because a reduced number of reassortant isolates were available for analysis of HA packaging preference.

Our reassortment data demonstrate that, when in competition within coinfected cells, the HA segment carrying heterologous packaging signals was usually excluded in favor of the HA segment carrying the better-matched, homologous, packaging signals. Corresponding packaging defects were observed when the heterologous HA segment was the only HA segment available for packaging, and in both cases the defect was more pronounced for HA_H5PS compared with HA_H7PS. Notably, however, the frequency of incorporation of the heterologous segments was lower in reassortant progeny viruses compared with clonal virus preparations, suggesting that competition between HA segments within coinfected cells exacerbated the packaging defects of HA_H5PS and HA_H7PS segments. Of note, we did not observe a difference in HA segment frequency in the concentrated HA_H3PS virus preparation compared with the control Pan/99 virus preparation, suggesting that the artificial lengthening of the HA_PS segments and the accompanying silent mutations did not disrupt HA packaging efficiency.

Given the relatively low incorporation of HA segments into virions, we were somewhat surprised by the lack of a growth defect of the HA_H5PS and HA_H7PS viruses compared with the HA_H3PS virus. The lack of detectable growth deficits may be attributable to the relatively small effect of the introduced sequences on packaging efficiency. In virions, the reduction in packaging of HA was approximately twofold for the HA_H5PS segment and 1.3-fold for the HA_H7PS segment. During growth under single-cycle conditions in cell culture or from a relatively high dose in vivo, these reductions in packaging efficiency may not be strong enough to markedly affect viral growth.

Limitations of our study include the absence of protein mismatch and the lack of preexisting immunity in our animal model. To isolate the effects of packaging signal mismatch on reassortment, we kept all proteins identical. In a natural setting, both the packaging signals and the proteins of the coinfecting viruses would differ and could constrain reassortment. Additionally, preexisting immunity to IAV is widespread in the human population, from natural infection and/or vaccination (22, 23). Our animal model does not recapitulate the immunological environment

that coinfecting viruses would encounter in a natural host, and preexisting immunity can play a major role driving the emergence of novel IAV reassortants (24, 25).

To date, the locations of the packaging signals on the eight IAV segments have been mapped largely within an H1N1 (WSN) virus (reviewed in ref. 26). We used a conservative estimate of the packaging signals determined for the H1 HA when designing our chimeric HA segments (27). Results obtained with the PSmut_HA segment suggest that the mutation strategy employed to disrupt native packaging function of the Pan/99 HA ORF did indeed target the H3 packaging signals. The residual level of incorporation of the PSmut_HA (~14%) is likely attributable to the presence of wild-type Pan/99 UTRs, which were left intact and have been shown to be involved in packaging in conjunction with the terminal coding regions (28, 29). It is also possible that sequences internal to the introduced mutations contribute to packaging.

A current gap in our knowledge of IAV genome incorporation relates to the network of interactions formed among the segments during the assembly process. During virus assembly, the eight segments are arranged into a "7 + 1" pattern, with one central segment surrounded by seven outer segments (30, 31). However, the identity of the segments in this pattern, which specific segments interact, and at what point during the viral life cycle the segments are bundled together, remain unclear. Further investigation of these points will help clarify not only the packaging process but also the role that packaging signal divergence plays in this process.

In summary, this work indicates that the likelihood of reassortment between human seasonal IAV and avian IAV is reduced by divergence in the RNA packaging signals of the HA segment. Nevertheless, HA segments carrying H5N8 or H7N9 packaging signals were incorporated into H3N2 viruses at a low level and, in the case of H5N8 packaging signals, propagated sufficiently in coinfected hosts to allow transmission to contact animals. These data will help to inform the reassortment potential of human and zoonotic IAV.

Materials and Methods

Design of Chimeric HA Segments and Virus Generation. Chimeric HA segments were designed as described previously (15, 16). Briefly, the introduced 3′ and 5′ packaging signal regions consisted of 136 nt derived from influenza A/mute_swan/Croatia/70/2016 (H5N8), influenza A/Anhui/1/2013 (H7N9), or Pan/99 (H3N2) HA segments. All chimeric segments and the PSmut_HA carried synonymous changes throughout 60 nucleotide regions adjacent to the start and stop codons. The PSmut_HA segment lacked introduced packaging signals. Viruses containing these modified HA segments were rescued in either a WT or VAR Pan/99 background as described previously (15). Our WT-VAR system outlined in ref. 17 consists of Pan/99 virus pairs that are either tagged with one to six silent mutations in each of the eight IAV segments (VAR) or untagged (WT). Genotyping can then be achieved by detecting the presence or absence of these mutations using high-resolution melt (HRM) analysis (32). HRM primers used can be found in *SI Appendix*, Table S1.

Virus Growth. MDCK cells were inoculated at a multiplicity of infection (MOI) of 5 pfu per cell in triplicate. Single-cycle replication conditions were achieved with ammonium chloride addition at 3 h p.i. Supernatants were sampled at 1, 4, 8, 12, 16, and 24 h p.i. and titered via plaque assay on MDCK cells. Guinea pigs were inoculated with 5×10^5 pfu of virus, four animals per virus. Nasal lavage was performed daily on day 1 through day 5 p.i., and samples were titered via plaque assay on MDCK cells.

Coinfection of MDCK Cells and Reassortment Analysis. MDCK cells were coinfected with WT-VAR virus pairs in triplicate (unless otherwise stated) as described previously (15). Briefly, an MOI of 10 pfu per cell for 1:1 WT:VAR infections was used to ensure high levels of coinfection (33), and virus replication was limited to a single cycle with ammonium chloride. Supernatants were harvested at 12 h p.i., and virus isolates were obtained by plaque purification on MDCK cells. For each sample, 21 plaques were picked randomly and genotyped as described previously (15). Briefly, quantitative PCR targeting each of the eight segments was performed and HRM analysis of amplicons was used to determine the parental origin of each segment in a given viral isolate.

Droplet Digital PCR to Evaluate vRNA Replication. To measure replication of the various modified HA segments over time, triplicate wells of MDCK cells were coinfected with 5 pfu per cell of each virus under single-cycle replication conditions. At 1, 4, 7, and 10 h p.i., coinfected cells and supernatants were harvested together as a single sample. RNA was extracted, converted to cDNA, and used in ddPCR (34) as described in ref. 15. Primers used were specific for the 3′ packaging signal region of each HA segment and showed no cross-priming. QuantaSoft software (Bio-Rad) was used to calculate HA copy numbers. ddPCR primers used can be found in *SI Appendix*, Table S2.

Reassortment and Virus Transmission in Guinea Pigs. All animal work was performed following the *Guide for the Care and Use of Laboratory Animals* (35) and was approved by the Emory Institutional Animal Care and Use Committee under protocol number DAR-2002738-ELMNTS-A. Intranasal inoculation and nasal lavage was performed as described previously (36). A 5×10^5 pfu mixture of WT and VAR virus diluted in PBS was used for the inoculation. Nasal wash samples of inoculated animals were processed for reassortment analysis in the same manner as the coinfection supernatants above. To evaluate transmission, RNA was extracted from contact animal nasal wash samples and converted into cDNA, and ddPCR was performed with 3′ HA packaging signal-specific primers to enumerate total HA copies as described above.

Quantification of vRNA in Concentrated Virus Preparations. Viruses were grown in embryonated eggs and pelleted through a 25% sucrose cushion. Resulting virus pellets were lysed, RNA was extracted, converted to cDNA, and used in ddPCR as described above with IAV segment-specific primers. The HA primers used were specific for a region of the HA segment conserved across all modified HA segments. IAV segment copy number was normalized to the corresponding PB2 copy number and then to the control Pan/99 values (also normalized to PB2). For quantification of the HA segment, two independent primer sets for both the HA and PB2 segments were used, and generated data were graphed separately.

Statistical and Sequence Analyses. Statistical analyses were performed in GraphPad Prism. Alignment of packaging signal sequences derived from IAV HA was performed using Clustal W.

ACKNOWLEDGMENTS. We thank Daniel Perez for the pDP2002 plasmid, Ketaki Ganti for assistance with animal experiments, and Nathan Jacobs for helpful discussion. This work was funded in part by the NIH/National Institute of Allergy and Infectious Diseases (NIAID) Centers of Excellence in Influenza Research and Surveillance (CEIRS), Contract HHSN272201400004C (to A.C.L. and J.S.) and by NIH/NIAID Grant R01 AI125268 (to A.C.L.).

1. Wright P, Neumann G, Kawaoka Y (2013) Orthomyxoviruses. *Fields Virology*, eds Knipe D, Howley P (Lippincott Williams & Wilkins, Philadelphia), 6th Ed, Vol 1.
2. Desselberger U, et al. (1978) Biochemical evidence that "new" influenza virus strains in nature may arise by recombination (reassortment). *Proc Natl Acad Sci USA* 75:3341–3345.
3. Kawaoka Y, Krauss S, Webster RG (1989) Avian-to-human transmission of the PB1 gene of influenza A viruses in the 1957 and 1968 pandemics. *J Virol* 63:4603–4608.
4. Smith GJD, et al. (2009) Origins and evolutionary genomics of the 2009 swine-origin H1N1 influenza A epidemic. *Nature* 459:1122–1125.
5. Kilbourne ED (2006) Influenza pandemics of the 20th century. *Emerg Infect Dis* 12:9–14.
6. Chan PK (2002) Outbreak of avian influenza A(H5N1) virus infection in Hong Kong in 1997. *Clin Infect Dis* 34(Suppl 2):S58–S64.
7. Gao R, et al. (2013) Human infection with a novel avian-origin influenza A (H7N9) virus. *N Engl J Med* 368:1888–1897.
8. Claas EC, et al. (1998) Human influenza A H5N1 virus related to a highly pathogenic avian influenza virus. *Lancet* 351:472–477.
9. Global Consortium for H5N8 and Related Influenza Viruses (2016) Role for migratory wild birds in the global spread of avian influenza H5N8. *Science* 354:213–217.
10. de Vries E, et al. (2015) Rapid emergence of highly pathogenic avian influenza subtypes from a subtype H5N1 hemagglutinin variant. *Emerg Infect Dis* 21:842–846.
11. Pohlmann A, et al. (2017) Outbreaks among wild birds and domestic poultry caused by reassorted influenza A(H5N8) clade 2.3.4.4 viruses, Germany, 2016. *Emerg Infect Dis* 23:633–636.
12. Lee DH, Bertran K, Kwon JH, Swayne DE (2017) Evolution, global spread, and pathogenicity of highly pathogenic avian influenza H5Nx clade 2.3.4.4. *J Vet Sci* 18:269–280.
13. Essere B, et al. (2013) Critical role of segment-specific packaging signals in genetic reassortment of influenza A viruses. *Proc Natl Acad Sci USA* 110:E3840–E3848.

14. Baker SF, et al. (2014) Influenza A and B virus intertypic reassortment through compatible viral packaging signals. *J Virol* 88:10778–10791.
15. White MC, Steel J, Lowen AC (2017) Heterologous packaging signals on segment 4, but not segment 6 or segment 8, limit influenza A virus reassortment. *J Virol* 91: e00195-17.
16. Gao Q, et al. (2012) The influenza A virus PB2, PA, NP, and M segments play a pivotal role during genome packaging. *J Virol* 86:7043–7051.
17. Marshall N, Priyamvada L, Ende Z, Steel J, Lowen AC (2013) Influenza virus reassortment occurs with high frequency in the absence of segment mismatch. *PLoS Pathog* 9: e1003421.
18. Ma EJ, Hill NJ, Zabilansky J, Yuan K, Runstadler JA (2016) Reticulate evolution is favored in influenza niche switching. *Proc Natl Acad Sci USA* 113:5335–5339.
19. Reperant LA, Kuiken T, Osterhaus AD (2012) Adaptive pathways of zoonotic influenza viruses: From exposure to establishment in humans. *Vaccine* 30:4419–4434.
20. White MC, Lowen AC (2018) Implications of segment mismatch for influenza A virus evolution. *J Gen Virol* 99:3–16.
21. Gamblin SJ, Skehel JJ (2010) Influenza hemagglutinin and neuraminidase membrane glycoproteins. *J Biol Chem* 285:28403–28409.
22. Gostic KM, Ambrose M, Worobey M, Lloyd-Smith JO (2016) Potent protection against H5N1 and H7N9 influenza via childhood hemagglutinin imprinting. *Science* 354: 722–726.
23. Hensley SE (2014) Challenges of selecting seasonal influenza vaccine strains for humans with diverse pre-exposure histories. *Curr Opin Virol* 8:85–89.
24. Ince WL, Gueye-Mbaye A, Bennink JR, Yewdell JW (2013) Reassortment complements spontaneous mutation in influenza A virus NP and M1 genes to accelerate adaptation to a new host. *J Virol* 87:4330–4338.
25. Mathews JD, McBryde ES, McVernon J, Pallaghy PK, McCaw JM (2010) Prior immunity helps to explain wave-like behaviour of pandemic influenza in 1918-9. *BMC Infect Dis* 10:128.
26. Hutchinson EC, von Kirchbach JC, Gog JR, Digard P (2010) Genome packaging in influenza A virus. *J Gen Virol* 91:313–328.
27. Watanabe T, Watanabe S, Noda T, Fujii Y, Kawaoka Y (2003) Exploitation of nucleic acid packaging signals to generate a novel influenza virus-based vector stably expressing two foreign genes. *J Virol* 77:10575–10583.
28. Fujii K, et al. (2005) Importance of both the coding and the segment-specific noncoding regions of the influenza A virus NS segment for its efficient incorporation into virions. *J Virol* 79:3766–3774.
29. Goto H, Muramoto Y, Noda T, Kawaoka Y (2013) The genome-packaging signal of the influenza A virus genome comprises a genome incorporation signal and a genome-bundling signal. *J Virol* 87:11316–11322.
30. Noda T, et al. (2006) Architecture of ribonucleoprotein complexes in influenza A virus particles. *Nature* 439:490–492.
31. Nakatsu S, et al. (2016) Complete and incomplete genome packaging of influenza A and B viruses. *MBio* 7:e01248-16.
32. Wittwer CT, Reed GH, Gundry CN, Vandersteen JG, Pryor RJ (2003) High-resolution genotyping by amplicon melting analysis using LCGreen. *Clin Chem* 49:853–860.
33. Fonville JM, Marshall N, Tao H, Steel J, Lowen AC (2015) Influenza virus reassortment is enhanced by semi-infectious particles but can be suppressed by defective interfering particles. *PLoS Pathog* 11:e1005204.
34. Schwartz SL, Lowen AC (2016) Droplet digital PCR: A novel method for detection of influenza virus defective interfering particles. *J Virol Methods* 237:159–165.
35. National Research Council (2011) Guide for the Care and Use of Laboratory Animals (National Academies Press, Washington, DC), 8th Ed.
36. Lowen AC, Mubareka S, Tumpey TM, García-Sastre A, Palese P (2006) The guinea pig as a transmission model for human influenza viruses. *Proc Natl Acad Sci USA* 103: 9988–9992.